

Electronic properties of TiSi₂ single crystals at low temperatures

M. Affronte

Istituto Nazionale per la Fisica della Materia and Dipartimento di Fisica, Università degli Studi di Modena, via G. Campi, 213/A, 41100 Modena, Italy

O. Laborde and J. C. Lasjaunias

Centre de Recherches sur les Très Basses Températures, Laboratoire associé à l'Université J. Fourier, Centre National de la Recherche Scientifique, Boîte Postale 166, 38042 Grenoble Cedex 9, France

U. Gottlieb and R. Madar

Laboratoire des Matériaux et du Génie Physique, Ecole Nationale Supérieure de Physique de Grenoble, Institut National Polytechnique de Grenoble, Boîte Postale 46, Domaine Universitaire, 38402 St. Martin d'Hères, France

(Received 4 March 1996)

We report measurements of Hall effect, transverse magnetoresistance, and specific heat on high-quality TiSi₂ (C54 phase) single crystals at low temperatures. We used crystals with low residual resistivity (typically $\rho_{4.2\text{ K}}=0.15\ \mu\Omega\text{ cm}$) and magnetic fields (B) up to 20 T. These facts allowed us to study the electronic properties from the low ($\omega_c\tau\ll 1$) to the high field regime ($\omega_c\tau>1$, $\omega_c=eB/m^*$ being the cyclotron frequency and τ the electron relaxation time) as a function of magnetic-field strength and temperature. The low field Hall coefficient R_H is negative, almost constant $R_H=-(0.5\pm 0.1)\times 10^{-10}\text{ m}^3/\text{C}$ between 100 and 300 K and it changes sign at ~ 30 K. The angular dependence of magnetoresistance shows either minima or maxima when the magnetic field is parallel to the principal crystallographic axes. These structures are, however, less pronounced than in other silicides, such as PdSi₂ and NbSi₂, and this suggests only a weak anisotropy of the TiSi₂ Fermi surface. The galvanomagnetic properties behave consistently with band-structure calculations of Mattheiss and Hensel [Phys. Rev. B **39**, 7754 (1989)] who found that TiSi₂ is a compensated metal with only closed orbits for the Fermi electrons. Using a simple two-band model we estimated, from the low field magnetoresistance, carrier density $n_e=n_h=(0.45-0.52)\times 10^{22}\text{ cm}^{-3}$ assuming equal concentration of electrons and holes. Low temperatures ($1.6<T<22\text{ K}$) specific-heat (C_p) measurements fit a linear $C_p/T=\gamma+\beta T^2$ dependence, with $\gamma=3.35\pm 0.05\text{ mJ/K}^2\text{ mol}$ and $\beta=0.0201\pm 0.0005\text{ mJ/K}^4\text{ mol}$. From these parameters we estimated the Debye temperature $\Theta_D=662\pm 4\text{ K}$ and the renormalized electronic density of states at the Fermi surface $N(\varepsilon_F)(1+\lambda)=2.85\text{ states/eV cell}$. [S0163-1829(96)02735-X]

INTRODUCTION

TiSi₂ is a material largely used for interconnects in silicon integrated circuit technology due to its low resistivity and its stability to heat treatments.¹ Studies on the formation of TiSi₂ thin films² have shown that there are two metallic orthorhombic phases: the base-centered C49 and the face-centered C54 phase. The latter is the most metallic and it can also be obtained as bulk single crystal. In the past few years, fundamental studies have been carried out on this material in order to better understand and to define the ultimate limits of its intrinsic properties. From an experimental point of view, however, most of the investigations have been performed on thin films.²⁻⁴ These generally are polycrystalline and therefore information on the anisotropy of the physical properties have been often neglected. Hall effect studies on TiSi₂ thin films have shown that R_H reverses sign at low temperatures.^{3,4} These studies were performed on films with a high residual resistivity and it was not unambiguously clarified whether the sign reversal was an intrinsic property of a compensated metal or it was simply due to the presence of the substrate. Furthermore, thin films are not suitable for the study of bulk properties such as specific heat.

Mattheiss and Hensel⁵ have recently performed electronic band-structure calculations. They found out that the C49 and C54 phase are compensated metals with both holelike and electronlike surfaces at the Fermi level. These authors have also found that the Fermi velocity can be rather anisotropic in the C54 phase. This may lead to some anisotropy of the electronic transport properties, a fact that is certainly important for several applications. Resistivity⁶ and preliminary optical investigations⁷ (no measurements were performed with the electrical field along the crystallographic c axis) showed only a rather weak anisotropy and much experimental effort is needed to clarify this aspect.

In this work we report measurements of the electronic properties performed on high quality TiSi₂ (C54 phase) single crystals (in the following we just name it "TiSi₂" without specifying that we deal with the C54 phase). The aim of this work is to gain more insight into the topology of the Fermi surface and to measure fundamental quantities such as the carrier density, the density of electronic states at the Fermi level, and the Debye temperature of this material. It is the first time, to our knowledge, that such a wide investigation has been performed on the electronic properties of this material.

EXPERIMENTAL TECHNIQUES AND DEFINITIONS

Electronic transport properties were measured by the 4-probe ac bridge method. Al wires, with diameter=25 μm , were soldered on samples by means of ultrasounds. Contacts are disposed in a linear array on bar shaped crystals used for magnetoresistance measurements. The Van der Pauw wire configuration was used for the $2 \times 1 \times 0.25 \text{ mm}^3$ crystals on which both Hall effect and magnetoresistance measurements were performed. The angular dependence of magnetoresistance was measured by using a cryogenic rotating sample-holder moved by an external computer controlled motor. For temperatures higher than liquid He, we used a capacitor thermometer for temperature stabilization.

The Hall voltage V_H is defined as the odd transversal voltage, i.e., $V_H = (V^+ - V^-)/2$ being V^+ and V^- the transverse voltage measured with the magnetic field (B) oriented in opposite directions. We then get the Hall resistivity $\rho_H = V_H t / I$, where t is the sample thickness, I the current, and also the odd transverse resistance $R_{TO} = V_H / I$. Using the same V^+ and V^- values we obtain the even transverse resistance $R_{TE} = (V^+ + V^-) / 2I$.

Specific-heat measurements were taken in a continuously operating pumped He-4 cryostat with sample in $\sim 10^{-6}$ torr vacuum. Heat capacity was measured by the quasiadiabatic method with typical temperature pulse $\Delta T \sim 1\%$ of the bath temperature.⁸

SAMPLE PREPARATION AND CHARACTERIZATION

The details of sample preparation and their characterization are reported in Ref. 6. Briefly, TiSi_2 single crystals were grown by a modified Czochralski technique from a levitated melt in a cold crucible, followed by an annealing at 900 °C in Ar atmosphere for 48 h. The orthorhombic crystalline structure (C54, space group $Fddd$) was checked by x-ray powder diffraction using Cr $K\alpha_1$ radiation with silicon as internal calibration standard. The measured lattice parameters were $a = 8.269 \text{ \AA}$, $b = 4.798 \text{ \AA}$, and $c = 8.552 \text{ \AA}$. In this work we present data obtained on samples used in our previous work⁶ (named ‘‘old’’) and also on samples recently grown (‘‘new’’). For magnetoresistance measurements we used ‘‘old’’ crystals having typical dimensions $1 \times 1 \times 5 \text{ mm}^3$. The longest dimension was taken parallel to one of the main crystallographic directions, the [100], [010], and the [001] axes. Subsequently we cut two 0.25-mm-thick and 2×1 -mm-wide samples from single crystal of the new batch and we used them for both Hall effect and magnetoresistance measurements. In this case, magnetic field was applied along the [100] and [010] crystallographic direction of the first and second crystal, respectively. Samples used in specific-heat measurements were also cut from new crystal and they are two 5-mm-thick cylinders with a total mass of 1.9879 g.

Resistivity

The detailed study of the temperature dependence of resistance measured in three bar shaped crystals was reported in our previous work.⁶ Here we briefly summarize the main results. Room-temperature resistivity was typically $\sim 10 \mu\Omega \text{ cm}$ and the residual resistivity ratio $\rho(293 \text{ K})/\rho(4.2 \text{ K})$ was between 50 and 80. The anisotropy of resistivity for

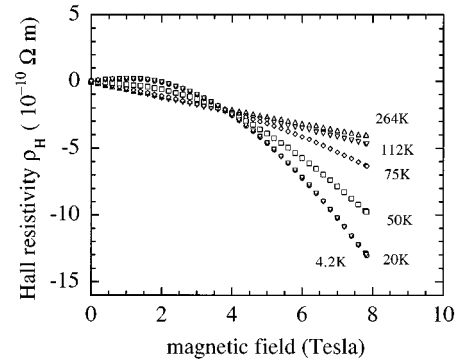


FIG. 1. Magnetic-field dependence of the Hall resistivity $\rho_H = (V_H/I)t$, where V_H is the odd transversal voltage, I the current, and t the crystal thickness, measured at different temperatures on TiSi_2 single crystal.

different crystallographic orientations was found smaller than 20%.⁶ Resistivity measurements on samples cut from the ‘‘new’’ crystals shows a resistivity ratio somewhat higher than the ‘‘old’’ crystals indicating an improvement of the crystal purity. Fitting the resistivity temperature dependence between 2 and 300 K with a conventional Bloch-Grüneisen curve we found a characteristic Debye temperature of 530 K.⁶ These values are in good agreement with transport properties measured in other single crystals by Hirano *et al.*⁹ and an almost identical value of Θ_D was also estimated by Sylla *et al.*¹⁰ by specific-heat measurements in the temperature range 100–500 K.

RESULTS

We have measured Hall effect and magnetoresistance between 4.2 K and room temperature as a function of magnetic field. We first report the magnetic-field dependence of these galvanomagnetic properties in order to distinguish different regimes of electron motion. According to the classification reported by Hurd,¹¹ the low field regime, in which electron orbits are not completed, is characterized by the condition $\omega_c \tau \ll 1$ while the high field regime is achieved when $\omega_c \tau \gg 1$, $\omega_c = eB/m^*$ being the cyclotron frequency and τ the electron relaxation rate. Subsequently we shall study the angular dependence of magnetoresistance in the high field limit, after which we shall report results obtained in the low field regime. Finally, low temperature specific-heat measurements will be reported.

Magnetic-field dependence of Hall effect and magnetoresistance

In Fig. 1 we show the magnetic-field dependence (up to 7.8 T) of the Hall resistivity ρ_H measured at different temperatures. At high temperature (264 K) ρ_H has a linear field dependence and it is entirely negative. As the temperature decreases, ρ_H is no more a linear function of magnetic field and, below $\sim 30 \text{ K}$, ρ_H is positive at low magnetic field (B), then it turns towards negative values as B increases. This nonlinear dependence of ρ_H on the magnetic field indicates that different regimes of the electron transport are crossed as the temperature is decreased. In order to better distinguish the different electron regimes, the same ρ_H data are replotted in Fig. 2 as a Kohler diagram. Namely, in Fig. 2 the Hall

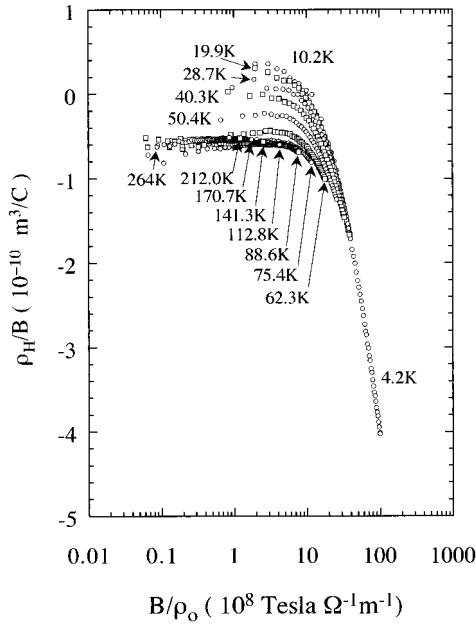


FIG. 2. Kohler diagram of the Hall resistivity ρ_H divided by the magnetic field B as a function of the reduced parameter B/ρ_0 (ρ_0 is the resistivity measured at zero field). ρ_H was measured at 14 different temperatures between 4.2 and 264 K. Data collected at 4.2 K were measured in magnetic field up to 20 T.

resistivity divided by the magnetic-field strength ρ_H/B is reported as a function of the reduced field B/ρ_0 , ρ_0 being the resistivity value measured at zero field. Also reported in this figure are data collected at 4.2 K and in magnetic field up to 20 T. We note that at high temperatures, as well as at sufficiently small magnetic field ($B/\rho_0 < 10^9 \text{ T } \Omega^{-1} \text{ m}^{-1}$), ρ_H/B is essentially field independent. In this case a Hall constant can be defined by the ρ_H/B ratio. Above the value $B/\rho_0 \sim 10^9 \text{ T } \Omega^{-1} \text{ m}^{-1}$ the quantity ρ_H/B is no more field independent and becomes more and more negative as the magnetic field increases. In the next graph, Fig. 3, we compare the

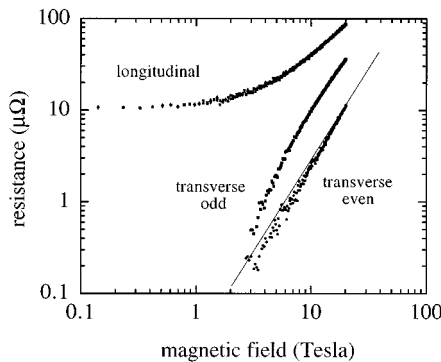


FIG. 3. Comparison between the odd transverse resistance $R_{\text{TO}} = (V^+ - V^-)/2I$ and the even transverse one $R_{\text{TE}} = (V^+ + V^-)/2I$ plotted as a function of magnetic field. We also report the longitudinal resistance measured on the same sample by aligning the voltage probes with the current ones. Note that in the case of the longitudinal resistance we plotted two curves (triangles up and down) obtained with magnetic field oriented in opposite directions: the two curves overlap each other as expected for a genuine magnetoresistance signal.

magnetic-field dependence of the odd transverse resistance R_{TO} with that of the even transverse component R_{TE} . We found that the even component is not negligible as compared with the odd one. Usually the former can be ascribed to the fact that the voltage probes are not perfectly aligned. In further experiment the voltage probes were aligned with those used for the current, in order to measure the magnetic-field dependence of genuine longitudinal voltage. Results are also reported in Fig. 3. We may notice that the behavior of the even transverse resistance is quite different as compared with that of the longitudinal component. Namely, the latter changes by a factor ~ 10 from 0 to 20 T and it saturates to a finite value at zero field while R_{TE} changes at least by a factor 50 from 0 to 20 T and it vanishes at zero field. We conclude that the even transverse field that we measured cannot be ascribed to the probe alignment, rather it seems to be an intrinsic property. We also note that R_{TE} goes as the squared magnetic field (represented by the unbroken line in Fig. 3) at the highest field.

Next we measured the magnetic-field dependence of the transverse magnetoresistance $\Delta\rho/\rho$ with the magnetic field oriented along the main crystallographic directions and perpendicular to the current. For these measurements we used both ‘‘new’’ and ‘‘old’’ crystals and a wide set of results obtained at 4.2 K and in magnetic fields up to 7.8 T was reported in Ref. 12. We found that the magnetoresistance keeps increasing in the whole range of magnetic-field strength for all the current and field orientations we have studied: no clear indication of saturation is observed. In Fig. 4 we report the transverse magnetoresistance $\Delta\rho/\rho$ as a function of the reduced field B/ρ_0 . In this plot we report the magnetoresistance measured at different temperatures on one of the ‘‘new’’ samples used also for Hall measurements. At $T=4.2$ K, measurements were performed in magnetic field up to 20 T. We observe that data obtained at different temperatures lie on the same curve indicating that the magnetoresistance is a function of the reduced parameter B/ρ_0 only, consistently with Kohler’s law. The straight line reported in Fig. 4 represents the B^2 behavior. We may notice that only at very low field ($B/\rho_0 < 10^9 \text{ T } \Omega^{-1} \text{ m}^{-1}$) the experimental data follow a B^2 behavior, while at higher field the magnetoresistance follows a power law weaker than B^2 . This behavior was also found for the other orientations of the magnetic field that we have studied. The absolute value of the magnetoresistance equals one at $B/\rho_0 \sim 2.6 \times 10^9 \text{ T } \Omega^{-1} \text{ m}^{-1}$. Similar value was found for the transverse magnetoresistance measured with other magnetic field and current directions. In particular, the magnetoresistance is ~ 1 for magnetic field ranging from 4 to 7 T at 4.2 K depending on field orientation.

In order to recognize different electron transport regimes, we compare the magnetic-field dependence of the Hall effect and magnetoresistance to the semiclassical theory of electron transport.^{11,13} In the simple case of a metal with two spherical surfaces of electrons and holes, one may find the simple relation $\Delta\rho/\rho \sim (\omega_c \tau)^2$.¹³ Here we assume that this relation holds also in our case and we use the magnetoresistance value to estimate $\omega_c \tau$. We found that $\Delta\rho/\rho$ equals one when the reduced field is $\sim 2.6 \times 10^9 \text{ T } \Omega^{-1} \text{ m}^{-1}$ (see Fig. 4). At 4.2 K and 20 T, $\Delta\rho/\rho$ is typically equal to 10. We note that in metallic silicides with higher resistivity ratio,^{14,15} we mea-

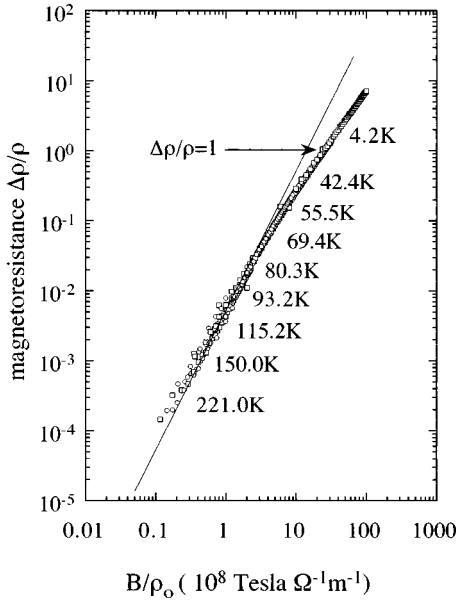


FIG. 4. Kohler diagram of the magnetoresistance $\Delta\rho/\rho$ as a function of the reduced parameter B/ρ_0 . Here, measurements were taken at 11 different temperatures between 4.2 and 221 K. Note that data collected at different temperatures lie on the same curve as predicted by the Kohler's law.

sured magnetoresistance values of the order of 10^2 at 7 T and 4.2 K. It is generally accepted that these magnetoresistance values guarantee that the high field regime is achieved in simple metals. In the case of TiSi_2 we may say that at $T=4.2$ K and $B=7$ T the high field regime is almost, but probably not completely, achieved. Consistently with this picture, we note that ρ_H/B is field independent for $B/\rho_0 < 10^9 \text{ T } \Omega^{-1} \text{ m}^{-1}$ (Fig. 2) and $\Delta\rho/\rho$ goes as B^2 as it is expected in the low field regime. We can also recognize that for $B/\rho_0 > 10^9 \text{ T } \Omega^{-1} \text{ m}^{-1}$ the observed behavior of the galvanomagnetic properties is quite close to what is expected for a compensated metal with no open orbits in the high field regime. According to the model developed by Fawcett for a compensated metal,¹³ one expects the appearance of even transverse resistance going as B^2 . This was actually observed in our experiments (see Fig. 3). The odd transverse component is expected to depend linearly on B , i.e., ρ_H/B should saturate. However, as Fawcett pointed out, one cannot exclude that terms of higher order in B may dominate the conductivity tensor and determine the odd transverse resistance of a compensated metal. This seems to be the case of TiSi_2 . Finally, in the high field regime the magnetoresistance is expected to increase as B^2 for a compensated metal.¹³ We have found that $\Delta\rho/\rho$ has a magnetic-field dependence weaker than B^2 for $B/\rho_0 > 3 \times 10^9 \text{ T } \Omega^{-1} \text{ m}^{-1}$. This may be due to the fact that the high field regime is almost, but not completely, achieved. However, several experimental artefacts are also known to mask a genuine B^2 dependence of magnetoresistance. Among these, crystal defects may add a linear term to the magnetic-field dependence of the magnetoresistance and probes not perfectly aligned may also alter the field dependence of $\Delta\rho/\rho$.¹³

Angular dependence of magnetoresistance

We have studied the angular dependence of magnetoresistance at different magnetic-field strengths and in several

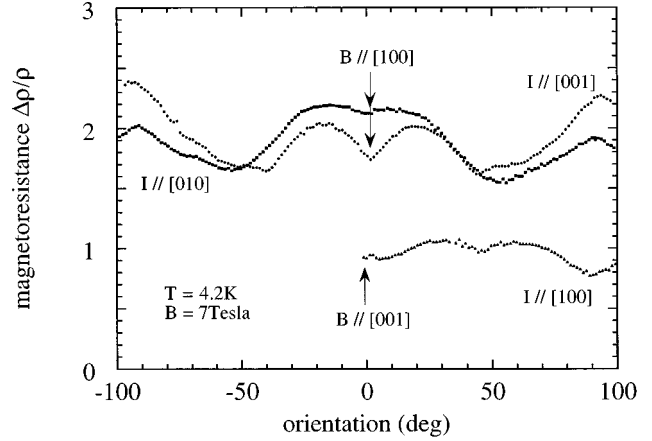


FIG. 5. Angular dependence of magnetoresistance measured on three oriented TiSi_2 single crystals at 4.2 K and $B=7$ T. The current (I) and magnetic field (B) directions with respect to crystallographic axis $[l m n]$ are specified for each curve. The orientation reported on the abscissa is the angle between the magnetic field B and the crystallographic axis at 0° in the plane perpendicular to the current direction.

crystals. A detailed study was reported in Ref. 12. We collected quite reproducible structures in all the samples we studied: Minima and maxima obtained for different magnetic-field strengths coincide in angle and they get more pronounced as the magnetic field increases, moreover samples with the same current and field orientations exhibit minima and maxima of $\Delta\rho/\rho$ at the same orientations.¹² In Fig. 5 we report the angular dependence of the transverse magnetoresistance measured in three TiSi_2 single crystals at 4.2 K in a magnetic field of 7 T, for which the high field regime is almost achieved, according to what we discussed before. The current (I) flows along the longest crystal direction that is specified for each crystal. The magnetic field (B) is always perpendicular to the current direction. The abscissa of this plot corresponds to the angle made by the magnetic field with the crystallographic axis specified for each curve. Minima and maxima are symmetric if we rotate the sample in opposite directions, i.e., curves obtained in the range $-90^\circ-0^\circ$ are symmetric to those obtained between 0° and 90° . Another feature of the curves reported in Fig. 5 is the fact that, when the magnetic field lies along the main crystallographic directions, we have either minima or maxima. This fact reflects the crystal symmetry. All these observations show that the curves reported in Fig. 5 reflect genuine features of the topology of the Fermi surface of this material.

Hall effect

Here we concentrate on the low field regime and we define the *low field* Hall coefficient R_H by taking the initial slope of the ρ_H vs B curves, i.e., $\partial\rho_H/\partial B$ at $B=0$, at any temperature. In Fig. 6 we plot the temperature dependence of the so defined R_H measured on two crystals. The Hall coefficient is almost temperature independent between 100 and 300 K, and is negative and its value is $R_H = -(0.5 \pm 0.1) \times 10^{-10} \text{ m}^3/\text{C}$ in both the crystals we measured. Below ~ 80 K the R_H absolute value decreases, R_H changes sign at ~ 30 K and becomes positive. Similar behav-

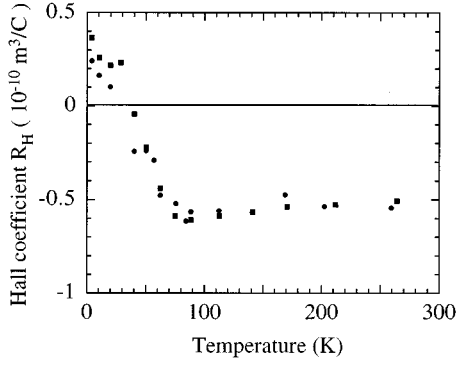


FIG. 6. Temperature dependence of the low field Hall coefficient, defined as $R_H = \partial \rho_H / \partial B$ at $B=0$ measured on two TiSi₂ single crystals having the magnetic field oriented along the [100] axis (circles) and [010] axis (squares), respectively. A change of sign is observed at ~ 30 K.

ior was also reported by Nava *et al.*,⁴ who measured the Hall coefficient of polycrystalline TiSi₂ thin films in magnetic fields up to 0.9 T. It is worth noting that the same R_H value was found on two differently oriented single crystals and in polycrystalline films above ~ 100 K. As R_H is a function of the σ_{ij} coefficients of the conductivity tensor,¹¹ the observed insensitivity of R_H to the magnetic-field orientation suggests that the Fermi surface of this material should be quite isotropic.

Specific heat

The heat capacity of two TiSi₂ cylinders cut from a single crystal rod was measured between 1.6 and 25 K. The specific heat of TiSi₂ was obtained by subtracting the heat capacity of addenda. This represents $\sim 25\%$ of the total heat capacity (TiSi₂ sample+addenda) at 10 K and it was previously determined with a precision of 5%. In Fig. 7 we plot the ratio of specific heat (C_p) over temperature C_p/T as a function of the squared temperature T^2 . Data lie in good approximation on a straight line. Using a conventional model, we can fit data with the curve

$$C_p/T = \gamma + \beta T^2,$$

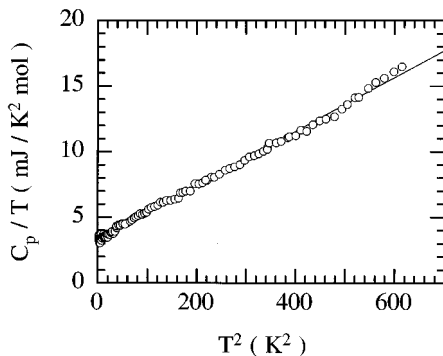


FIG. 7. Low-temperature specific heat C_p measured on TiSi₂ single crystal. Data are plotted as C_p/T vs T^2 to show that the $C_p = \gamma T + \beta T^3$ dependence is observed up to 22 K.

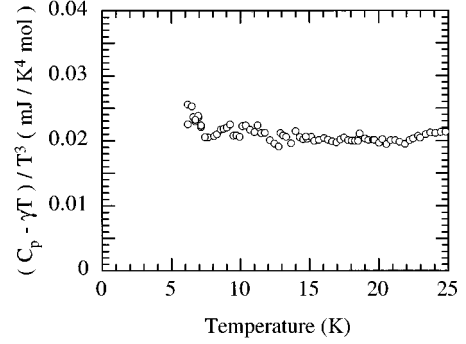


FIG. 8. Temperature dependence of the specific-heat lattice contribution ($C_p - \gamma T$) divided by T^3 measured on TiSi₂ single crystal. No deviation from the Debye T^3 law is observed between 5 and 22 K.

where γ is the Sommerfeld electronic term and β represents the lattice contribution to specific heat. From data fitting we obtain

$$\gamma = 3.35 \pm 0.05 \text{ mJ/K}^2 \text{ mol},$$

$$\beta = 0.0201 \pm 0.0005 \text{ mJ/K}^4 \text{ mol}.$$

Taking experimental data up to 22 K, the γ and β values do not depend on the temperature range used for fitting, at least within the specified accuracy. Note, however, that data precision gets lower below 4 K and the error on the determination of the γ and β values consequently increases. The lattice contribution was evaluated by subtracting the linear term γT to the total TiSi₂ specific-heat data. In Fig. 8 we plot $(C_p - \gamma T)/T^3$ as a function of temperature, in order to see to what extent β is temperature independent. $(C_p - \gamma T)/T^3$ does not depend on temperature, within our experimental precision, and no bumps are evident in the temperature range 5–22 K. At the highest temperature, i.e., close to 25 K, there is a small $(C_p - \gamma T)/T^3$ increase indicating a departure from the simple T^3 law. Using the standard formula

$$\beta = \frac{12}{5} r R \frac{\pi^4}{\Theta_D^3}$$

(with R the gas constant and r the number of ions per molecule) we can determine a mean Debye temperature. Taking $r=3$, we find $\Theta_D = 662 \pm 4$ K. In this case we assumed that the Debye model takes into account the $3rN$ phonon modes (acoustic+optical). However, another possibility is to take $r=1$ for the definition of the Debye temperature Θ_D^{ac} . In this case, the Debye model takes into account only the acoustic modes. With $r=1$ we have $\Theta_D^{\text{ac}} = 459 \pm 3$ K. Obviously, the two assumptions give the same βT^3 contribution to specific heat at low temperature but they differ for the Dulong and Petit saturation value that in one case ($\Theta_D = 662$ K) is $3rR$ while for $\Theta_D^{\text{ac}} = 459$ K is $3R$. This is illustrated in Fig. 9, where the Debye curves with $\Theta_D = 662$ K and $\Theta_D^{\text{ac}} = 459$ K are plotted up to saturation. It should also be pointed out that the simple T^3 lattice contribution is expected for temperature much smaller than Θ_D . In our case the T^3 law is observed up to 22 K, which corresponds to $\sim \Theta_D^{\text{ac}}/20$ and this makes the evaluation of Θ_D^{ac} self-consistent.

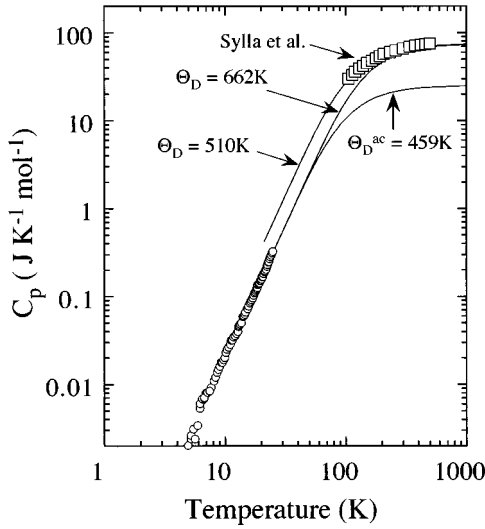


FIG. 9. Comparison between low-temperature (circles) and high-temperature (squares, data from Ref. 10) specific heat of TiSi_2 . Continuous lines were calculated by using the specific-heat expression of the Debye model with three different Debye temperatures $\Theta_D = 662, 510$, and 459 K, respectively. Note that the curves with $\Theta_D = 662$ K and $\Theta_D^{\text{ac}} = 459$ K, calculated taking the number of ions $r=3$ and 1 , respectively, correspond to the same low-temperature βT^3 term. Note also that the curves with $\Theta_D = 662$ K and 510 K saturate at the same Dulong and Petit value $3rR = 74.8$ $\text{J K}^{-1} \text{mol}^{-1}$.

The linear term of specific heat can be interpreted by using the conventional Sommerfeld theory of a free-electron gas:

$$\gamma = \frac{\pi^2 k_B^2 N_A}{3n} N(\epsilon_F)(1 + \lambda),$$

where γ is in $\text{eV/K}^2 \text{mol}$, n is the number of molecules per unit cell ($n=2$ in the case of TiSi_2), $N(\epsilon_F)$ is the density of electronic states expressed in states/eV cell, N_A and k_B the Avogadro number and the Boltzmann constant, respectively, $(1 + \lambda)$ is the renormalization factor that takes into account the electron phonon coupling. We found $N(\epsilon_F)(1 + \lambda) = 2.85$ states/eV cell.

DISCUSSION

Electronic band-structure calculations for TiSi_2 have been recently reported by Mattheiss and Hensel.⁵ Band structure are characterized by low-lying Si $3s$ - $3p$ bands and partially filled Ti $3d$ bands. The calculated C54 Fermi surface consists of several closed sheets including a single electron pocket at Γ as well as three nested hole surfaces. It turns out from these calculations that TiSi_2 is a compensated metal having an equal number of electrons and holes. In the first part of this work we have shown that the behavior of TiSi_2 is consistent with that of a compensated metal with only closed orbit. Based on these experimental results and on band-structure calculations we use a simple two-band model to determine the main physical quantities. In the low field regime, the expression of magnetoresistance and Hall effect for a compensated metal are¹⁶

$$R_H = \frac{(\sigma_e^2 R_{He} + \sigma_h^2 R_{Hh})}{\sigma^2},$$

$$\frac{\Delta\rho}{\rho} = \alpha \left(\frac{B}{\rho} \right)^2 \quad \text{with} \quad \alpha = \frac{(\sigma_e \mu_e^2 + \sigma_h \mu_h^2)}{\sigma^3},$$

where σ_x are the conductivities, μ_x the mobilities, and $R_{Hx} = 1/qn_x$ ($q = \pm e$ is the charge and n_x the carrier density) are the Hall coefficient contributions of electrons (e) and holes (h). In the formula reported above, we consider only the linear field dependence of ρ_H and the quadratic dependence of magnetoresistance and we neglected contributions of higher order in magnetic field. We note that the expression of the Hall coefficient is extremely sensitive to the ratio μ_e/μ_h between the hole and electron mobilities, while the α coefficient of magnetoresistance is affected very little by small changes of μ_e/μ_h . Resistivity of TiSi_2 follows a Bloch-Grüneisen temperature dependence⁶ and this indicates that carriers are scattered by phonons at high temperature and defects at low temperature. Thus it is likely that electron and holes are scattered in a different manner as the temperature is lowered. As a consequence, the μ_e/μ_h ratio is expected to be temperature dependent. That is the origin of the change of the R_H sign. On the other hand, we may simply assume that $n_e = n_h$ and $\mu_e = \mu_h$ for magnetoresistance as the latter is not sensitive to small variations of μ_e/μ_h ratio. From the measured value of $\alpha = (35-50) \times 10^{-20} \text{ m}^6/\text{C}^2$ we can estimate the density of charge carriers $n_e = n_h = (0.45-0.52) \times 10^{22} \text{ cm}^{-3}$. This can be compared with the value $(0.62) \times 10^{22} \text{ cm}^{-3}$ estimated by band-structure calculations.⁵ The agreement is quite good.

According to Kohler's rule one may expect to find that $\Delta\rho/\rho$ and ρ_H/B data obtained at different temperatures overlap when plotted as a function of the reduced field B/ρ_0 making continuous lines. This rule, however, is obeyed under the condition that a temperature change alters all the relaxation times $\tau(k)$ by the same factor.¹³ As we noted above, in the case of TiSi_2 the μ_e/μ_h ratio significantly changes at low temperature, thus it is not surprising to observe that the ρ_H/B data do not overlap in Fig. 2. Magnetoresistance is less sensitive to μ_e/μ_h variations, according to what we discussed before, thus the fact that $\Delta\rho/\rho$ data form more or less a continuous line in Fig. 4 does not imply that Kohler's conditions are respected.

The study of the magnetic-field dependence of magnetoresistance, with current and magnetic field along the principal crystallographic directions, has never shown indications for magnetoresistance saturation. The latter is generally considered as an indication for the presence of open orbits. Although we cannot rule out the possibility to have open orbits in particular crystallographic directions, these features of magnetoresistance are consistent with band-structure calculations that show only closed Fermi surfaces.

The angular dependence of magnetoresistance shows the presence of maxima or minima along the principal crystallographic directions. Although the magnetoresistance is not simply related to the topology of the Fermi surface, we can certainly say that curves of Fig. 5 reflect the anisotropy of the electronic bands. We can observe, however, that the relative difference between minima and maxima of $\Delta\rho/\rho$ shown in Fig. 5 is relatively weak if we compare them with what we

obtained in other silicides, such as Pd₂Si (Ref. 14) and NbSi₂.¹⁵ In other words, the angular dependence of magnetoresistance is rather smooth for TiSi₂. This suggests that the Fermi surface of this material is quite isotropic. This is consistent with the weak anisotropy that we found in the TiSi₂ resistivity tensor.⁶ Furthermore, we found almost identical Hall behavior in two single crystals differently oriented and in polycrystalline films indicating once more weak anisotropy. Band-structure calculations,⁵ on the other hand, gave quite different values of the Fermi velocity along different crystallographic directions. This would imply a quite anisotropic resistivity tensor in disagreement with the experimental results reported in this work. New band-structure calculations¹⁷ give a more isotropic Fermi velocity, a picture that is more consistent with our experimental results.

From specific-heat measurements we determine the Debye temperature $\Theta_D = 662 \pm 4$ K taking $r=3$ and $\Theta_D^{\text{ac}} = 459 \pm 3$ K with $r=1$. Fitting the temperature dependence of resistivity with Bloch-Grüneisen curve we have estimated that $\Theta_D = 535 \pm 10$ K in a previous work.⁶ Recent specific-heat measurements in the temperature range 100–500 K gave an estimation of $\Theta_D = 510$ K.¹⁰ In Fig. 9 we compare the low-temperature lattice contribution to specific heat ($C_p - \gamma T$) with data obtained by Sylla and co-workers¹⁰ at high temperature. In this plot we also report three Debye curves which have characteristic Θ_D equal to 510, 662, and 459 K, respectively. As previously discussed, both curves with $\Theta_D = 662$ and 459 K fit well the lattice contribution at low temperature. Yet, the curve with $\Theta_D^{\text{ac}} = 459$ K does not take into account all the phonon modes (we took $r=1$) and therefore it does not give the right value of the specific heat at high temperature. The Debye curve with $\Theta_D = 662$ K takes into account $3rN$ phonon modes and gives the right Dulong and Petit value $3rR$ of the high-temperature specific heat. Due to the oversimplified approximation, however, the Debye model is only a very rough approximation of the actual phonon spectrum and the curve with $\Theta_D = 662$ K does not fit well, although it is close to the high-temperature specific-heat data. On the other hand, if we use high-temperature data to determine Θ_D , we obtain a mean value (510 K) that averages the effects of the phonon modes active at high temperature. Thus, it is not surprising that the corresponding Debye curve does not fit our data at low temperature where only the acoustic branches are active.

With our measurement of β we can estimate the mean Debye sound velocity of this material. Using the relation

$$\frac{C_p}{T^3} = \frac{2\pi^2 k_B^4}{5 \hbar^3} \frac{1}{\rho v_D^3}$$

and taking the density $\rho = 4.08 \text{ g cm}^{-3}$, we estimate $v_D = 5370 \text{ ms}^{-1}$.

From the linear γ term of the specific heat we calculated the renormalized electronic density of states at the Fermi surface $N(\varepsilon_F)(1+\lambda) = 2.85$ states/eV cell. This can be compared with that reported by Mattheiss and Hensel,⁵ that is, $N(\varepsilon_F) = 2.42$ states/eV cell. The density of electronic states measured by low-temperature specific heat is somewhat higher than that obtained by band-structure calculations. The difference may be due to the renormalization term, i.e., the electron-phonon coupling factor $(1+\lambda)$. If we directly compare the two results it turns out that λ should be equal to 0.18. This value is somewhat smaller than what we found in TaSi₂ (Ref. 18) and NbSi₂,¹⁹ which are superconducting at low temperature.

In conclusion, we have measured different electronic properties of TiSi₂ single crystals at low temperatures. The low field Hall effect exhibits a change of sign at ~ 30 K, and we showed that this can be considered a typical behavior of a compensated metal. The angular dependence of transverse magnetoresistance shows only a weak anisotropy and the $\Delta\rho/\rho$ magnetic-field dependence is consistent with a model of compensated metal with only closed electron and hole orbits. From low field magnetoresistance data we have estimated the carrier density $n_e = n_h = (0.45 - 0.52) \times 10^{22} \text{ cm}^{-3}$ using a simple two-band model and assuming equal number and mobility for electrons and holes. The specific heat of TiSi₂ single crystals follows a simple $C_p = \gamma T + \beta T^3$ temperature dependence with $\gamma = 3.35 \pm 0.05 \text{ mJ/K}^2 \text{ mol}$ and $\beta = 0.0201 \pm 0.0005 \text{ mJ/K}^4 \text{ mol}$ between 1.6 and 22 K. From these values we estimate the mean Debye temperature $\Theta_D = 662 \pm 4$ K and the renormalized electronic density of states at the Fermi surface $N(\varepsilon_F)(1+\lambda) = 2.85$ states/eV.

ACKNOWLEDGMENTS

We thank Dr. A. Rouault and Dr. Yang Hongshun for their help on sample preparation and specific-heat measurements, respectively. This work was financially supported by the European Community in the framework of the program Human Capital and Mobility, Contract No. ERBCHRXTCT930318.

¹K. Maex, Phys. World **8**, 35 (1995).

²J. C. Hensel, J. M. Vandenberg, F. C. Unterwald, and A. Maury, Appl. Phys. Lett. **51**, 1100 (1987).

³B. Z. Li, A. M. Zhang, G. B. Jiang, R. G. Aitken, and K. Daneshvar, J. Appl. Phys. **66**, 5416 (1989).

⁴F. Nava, K. N. Tu, E. Mazzega, M. Michelini, and G. Queirolo, J. Appl. Phys. **61**, 1085 (1987).

⁵L. F. Mattheiss and J. C. Hensel, Phys. Rev. B **39**, 7754 (1989).

⁶O. Thomas, R. Madar, J. P. Senateur, and O. Laborde, J. Less-

Common Met. **136**, 175 (1987).

⁷M. Tanaka, S. Kurita, F. Fujisawa, and F. Levy, Phys. Rev. B **43**, 9133 (1991).

⁸F. Zougmore, J. C. Lasjaunias, and O. Béthoux, J. Phys. (France) **50**, 1241 (1989).

⁹T. Hirano and M. Kaise, J. Appl. Phys. **68**, 627 (1990).

¹⁰W. K. Sylla, S. E. Stillman, M. S. Sabella, and E. J. Cotts, J. Appl. Phys. **76**, 2752 (1994).

¹¹C. M. Hurd, *The Hall Effect in Metals and Alloys* (Plenum Press, New York, 1972).

- ¹²M. Affronte, O. Laborde, U. Gottlieb, O. Thomas, and R. Madar, *Appl. Surf. Sci.* **91**, 98 (1995).
- ¹³E. Fawcett, *Adv. Phys.* **13**, 139 (1964).
- ¹⁴U. Gottlieb, O. Laborde, and R. Madar, in *MRS Symposia Proceedings No. 320* (MRS, Pittsburgh, 1994), p. 473.
- ¹⁵O. Laborde, U. Gottlieb, and R. Madar, *J. Low Temp. Phys.* **95**, 835 (1994).
- ¹⁶J. M. Ziman, *Principles of the Theory of Solids*, 2nd ed. (Cambridge University Press, Cambridge, 1972).
- ¹⁷Victor Antonov and Vladimir Antonov (private communication).
- ¹⁸U. Gottlieb, J. C. Lasjaunias, J. L. Tholence, O. Laborde, O. Thomas, and R. Madar, *Phys. Rev. B* **45**, 4803 (1992).
- ¹⁹J. C. Lasjaunias, O. Laborde, U. Gottlieb, R. Madar, and O. Thomas, *J. Low Temp. Phys.* **92**, 335 (1993).